Upper mantle Q and thermal structure beneath Tanzania, East Africa from teleseismic P wave spectra

Anupama Venkataraman,[1] Andrew A. Nyblade,[2] and Jeroen Ritsema[3]

Received 25 April 2004; revised 3 July 2004; accepted 13 July 2004; published 7 August 2004.

[1] We measure P wave spectral amplitude ratios from deep-focus earthquakes recorded at broadband seismic stations of the Tanzania network to estimate regional variation of sublithospheric mantle attenuation beneath the Tanzania craton and the eastern branch of the East African Rift. One-dimensional profiles of Q_P adequately explain the systematic variation of P wave attenuation in the sublithospheric upper mantle: $Q_P \sim 175$ beneath the cratonic lithosphere, while it is ~ 80 beneath the rifted lithosphere. By combining the Q_P values and a model of P wave velocity perturbations, we estimate that the temperature beneath the rifted lithosphere (100–400 km depth) is 140–280 K higher than ambient mantle temperatures, consistent with the observation that the 410 km discontinuity in this region is depressed by 30–40 km. *INDEX TERMS:* 3909 Mineral Physics: Elasticity and anelasticity; 7203 Seismology: Body wave propagation; 7218 Seismology: Lithosphere and upper mantle; 8109 Tectonophysics: Continental tectonics—extensional (0905); 8124 Tectonophysics: Earth's interior—composition and state (1212). **Citation:** Venkataraman, A., A. A. Nyblade, and J. Ritsema (2004), Upper mantle Q and thermal structure beneath Tanzania, East Africa from teleseismic P wave spectra, *Geophys. Res. Lett.*, *31*, L15611, doi:10.1029/2004GL020351.

1. Introduction

[2] East Africa is a geologically unique region with Cenozoic volcanism and a developing continental rift system that is impinging on cratonic lithosphere. Many studies using data from the 1994–1995 Tanzania network of broadband seismometers (Figure 1) have provided insights into the formation of the eastern and western branches of the Cenozoic East African Rift (EAR) that encircle the Archean Tanzania Craton (Figure 1) [*Nyblade*, 2002]. This PASSCAL network was comprised of 20 broadband seismometers located along two arrays (EW and NE-SW) across the Tanzania craton and the adjacent rifts [*Owens et al.*, 1995], and operated between June 1994 and May 1995. Heat flow measurements [*Nyblade*, 1997], teleseismic P and S [*Ritsema et al.*, 1998] and Pn velocity tomography [*Brazier et al.*, 2000], receiver functions studies of crustal [*Last et al.*, 1997] and mantle transition zone structure [*Owens et al.*, 2000] indicate: a) that the crustal thickness varies from 37–42 km beneath the Tanzania stations, b) that the lithospheric keel of the Tanzania craton extends to at least 170 km depth [*Weeraratne et al.*, 2003], and c) that temperatures are elevated by 200–300 K beneath the eastern rift at about 400 km depth [*Owens et al.*, 2000]. *Nyblade* [2002] attributed the anomalously low seismic velocities and elevated temperatures beneath the eastern rift to a mantle plume.

[3] Temperature anomalies inferred from velocity anomalies can be overestimated if anelasticity is not considered [*Karato*, 1993]. Anelasticity is strongly temperature dependent and can contribute significantly to changes in velocity caused by temperature variations in the mantle [*Cammarano et al.*, 2003]. To better constrain the thermal anomaly beneath the eastern rift, we analyze P wave attenuation beneath the Tanzania seismic network and the adjacent rift system and interpret our estimates of Q_P in combination with P wave velocity anomalies determined from seismic tomography [*Ritsema et al.*, 1998].

2. Measurement of Attenuation

2.1. Data

[4] We analyze P waves generated by large ($M_W \geq 6.0$) teleseismic earthquakes at distances between 30° and 90° recorded by the Tanzania array. We chose deep earthquakes (>200 km) so that the direct P wave arrivals are not complicated by surface reflections (i.e., pP, sP) nor attenuated by the uppermost mantle at the source. During the operation of the Tanzania network, two events in Indonesia and two events in the Hindu Kush region rendered recordings of sufficiently high quality. The proximity and similarity of the source mechanism of the earthquakes in each pair allows us to check for consistency in our measurements.

[5] We use 35 seconds of data windowed around the theoretical arrival time of the direct P wave. Figure 2a shows the P wave velocity spectra and the noise spectra at three stations from one of the deep Java sea events. High signal-to-noise ratios at frequencies between 0.05 and 1 Hz are typical for data at most stations. We smooth the amplitude spectra for each station by computing a running average over a moving window of width 25 percent of the frequency range (0.07–0.45 Hz) to remove spectral holes.

2.2. Method

[6] The amplitude of the observed spectrum $O(\omega)$ at a station can be written in terms of the source spectrum $S(\omega)$, crustal response $C(\omega)$ and attenuation along the path $A(\omega)$ as:

$$O(\omega) = S(\omega)C(\omega)A(\omega) = S(\omega)C(\omega)e^{-\omega t^*/2} \quad (1)$$

[1]Department of Geophysics, Stanford University, Stanford, California, USA.
[2]Department of Geosciences, Pennsylvania State University, University Park, Pennsylvania, USA.
[3]Laboratoire de Sismologie, Institut de Physique du Globe, Paris, France.

0094-8276/04/2004GL020351$05.00

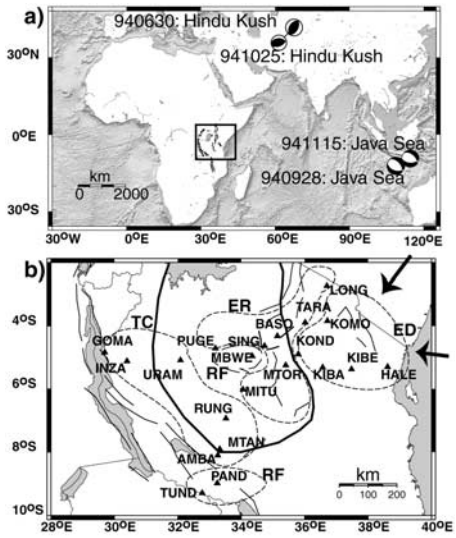

Figure 1. a) Map showing the location and focal mechanisms of the four teleseismic events used in this study. The rectangle marks the study area. b) The outline of the Tanzania craton (bold line) and surrounding rift faults (lighter black lines), and the PASSCAL station locations (solid triangles). We exclude stations MTAN and INZA from our analysis because of instrument malfunctions [*Langston et al.*, 2002]. The arrows indicate the azimuth of the incoming rays from the Hindu Kush and Java sea events. The dashed lines outline stations that receive rays traversing the upper mantle through the Tanzania craton region (TC), the edge of rift region (ER), rift region (RF) and edge region (ED).

where $t^* = \int_{path} \frac{dT}{Q}$ is the attenuation constant, dT is the travel time along the ray path, Q is the quality factor that quantifies the dissipation of seismic energy in the earth, and $\omega = 2\pi f$, where f is frequency in Hz. Because the crustal structure is fairly uniform for all stations [*Last et al.*, 1997], we can relate the natural logarithm of the spectral ratio $R(\omega)$ for the same earthquake recorded at stations i and j in a linear fashion:

$$\ln R_{ij}(\omega) = \ln\big(O_i(\omega)/O_j(\omega)\big) = -\omega\big(t_i^* - t_j^*\big)/2 = -\omega\Delta t_{ij}^*/2 \tag{2}$$

To determine Δt_{ij}^* from data, we fit a straight line for the spectral ratios for each pair of stations using least squares. We can determine Δt_{ij}^* from the slope of this straight line. Spectral ratios for three stations shown in Figure 2a are plotted as a function of frequency in Figure 2b.

[7] We make $n(n-1)/2$ measurements of Δt_{ij}^* (i.e., for all station pairs) and apply a distance correction to the Δt_{ij}^* values using the IASP91 model [*Kennet and Engdahl*, 1991]. With the constraint equation $\sum_{i=1}^{n} t_i^* = 0$ that sets (arbitrarily) the mean t^* to zero, we estimate relative t^* for each station using the multi-channel cross-correlation method of *VanDecar and Crosson* [1990], originally applied to teleseismic travel times.

[8] Figure 3 shows the variation in relative t^* values along the two profiles for one event in each pair. There is a systematic variation in relative t^* values from east to west along the EW profile. P waves recorded at stations to the west of the rift are attenuated more than P waves recorded further east, since they propagate a longer distance through the rift. This trend follows, to the first order, the trend observed in P wave velocity [*Ritsema et al.*, 1998]. The nearly identical t^* values for events in the same region demonstrate that our measurements are robust.

3. Modeling the Attenuation Structure

[9] Our data set is too small to be directly inverted for vertical and lateral variations of Q_P in the region. Therefore, we parameterize a model of Q_P with four 1D profiles that consist of lithosphere overlying a sub-lithospheric mantle to 450 km depth. The thickness of the lithosphere is imaged best by the seismic velocity studies in the region (see *Nyblade* [2002] and references therein) and is held fixed in our models. We also fix Q_P of the lithosphere at 1450 (the value in PREM, *Dziewonski and Anderson* [1981]); varying the Q_P value from 500 to 1450 has little effect on the results. We do not account for the frequency dependence of Q_P, and ignore scattering and focusing effects.

[10] Figure 4a shows schematically the upper mantle structure of four terrains in the region with fixed lithospheric thickness given in Table 1 from the interpretation of *Nyblade* [2002]: (1) the Tanzania Craton (region TC), (2) the edges of the rift (region ER), (3) the Eastern and Western Rift (region RF) and (4) the edge region (region ED). The

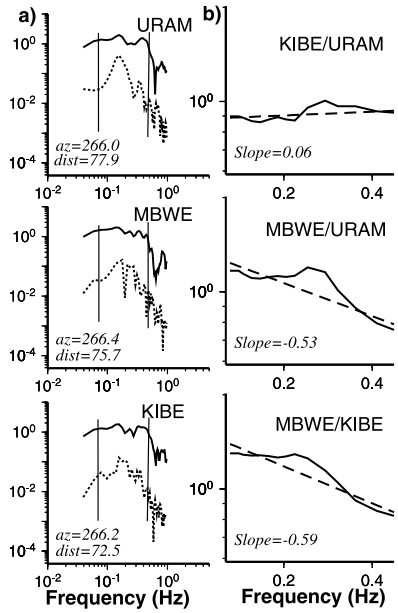

Figure 2. a) P wave velocity spectrum (top trace) and noise spectrum (dashed line) at three stations for the 940928 Java Sea event. The station azimuth (az) and distance (dist) to the earthquake both in degrees are shown on each plot. Data between the thin lines (0.07 Hz–0.45 Hz) was used to calculate the spectral ratios; b) Solid lines show the spectral ratios of station pairs (station names are indicated at the top). The dashed line is the least squares fit to the spectral ratio in each case and the slope of the straight line is indicated on the plot. The error in the individual spectral fits is <6%.

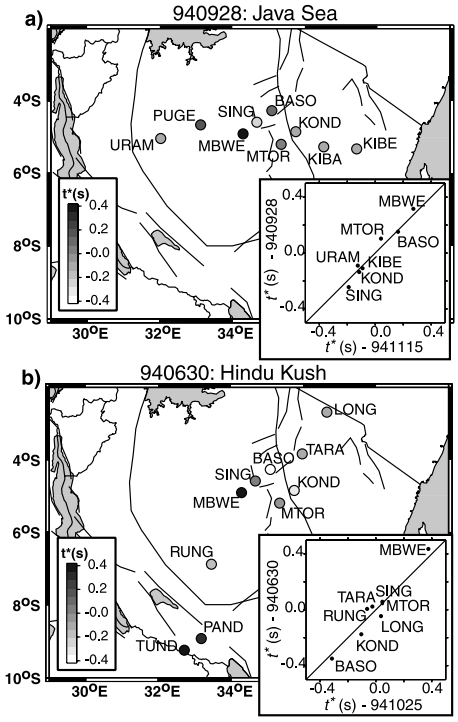

Figure 3. Relative t^* values at stations; the scale on the left shows the variation in relative t^* from negative (low t^*, low attenuation) shown in white to positive (high t^*, large attenuation) shown in black. Inset shows the comparison between the relative t^* values for the earthquakes in each pair: a) 940928: Java Sea event; b) 940630: Hindu Kush event. The good correlation (0.98 and 0.97 respectively) in the relative t^* values shows that our measurements are robust.

relative t^* of regions (1), (2), and (3) requires an average attenuation larger than PREM. We consider the position of the station within Tanzania to determine which of the four terrains is responsible for the observed attenuation. Since the P wave propagates through the upper mantle with a 20°–30° angle of incidence, it samples the portion of the upper mantle that is within 200 km of the station. For example, P waves traveling from the Java events to station

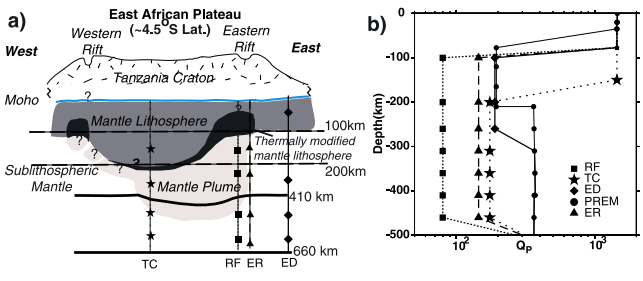

Figure 4. a) Schematic model of upper mantle structure derived from body and surface wave velocity data from *Nyblade* [2002]. The vertical lines through the model show the locations of the different terrains. The horizontal dashed lines indicate the lithospheric thickness. b) Variation of attenuation (Q_P) with depth for the different terrains obtained from modeling the relative t^* variations.

Table 1. Attenuation Model

		TC	ER	RF	ED
Lithosphere	Thickness (km)	200	100	100	100
	Q_P	1450	1450	1450	1450
Sub-lithosphere	Best LSQ fit is obtained for Q_P varying between	145–205	135–155	80–90	160–210
	Preferred Q_P values	175	145	80	190

BASO propagate through the ED structure, while P waves traveling from the Hindu Kush events to station BASO propagate through the ER structure.

[11] Using a grid-search, we determined Q_P in the sublithospheric mantle in each of the four regions. We vary Q_P from 215 to 40 for the TC, ER, RF and ED regions in increments of 5. The best least squares fit for Q_P in the different regions and the Q_P values that best fit all the data (our preferred Q_P values for the sublithosphere) are shown in Table 1. These best Q_P model, also shown in Figure 4b), is used to calculate the model t^* values that are compared to the measured values in Figure 5). Our simple model cannot explain the data at stations SING and BASO that lie in the region where the eastern rift intersects the craton and disrupts the structure of the region.

4. Discussion

[12] The good fit (Figure 5) suggests that to the first order simple 1D models of Q_P explain the observed variation in relative t^*. We find that the region below the lid has a $Q_P \approx 80$ in the rift zone (RF) whereas for the craton (TC) $Q_P \approx 175$ between 200–450 km depths. The relatively low value of Q_P beneath the rift is consistent with the low

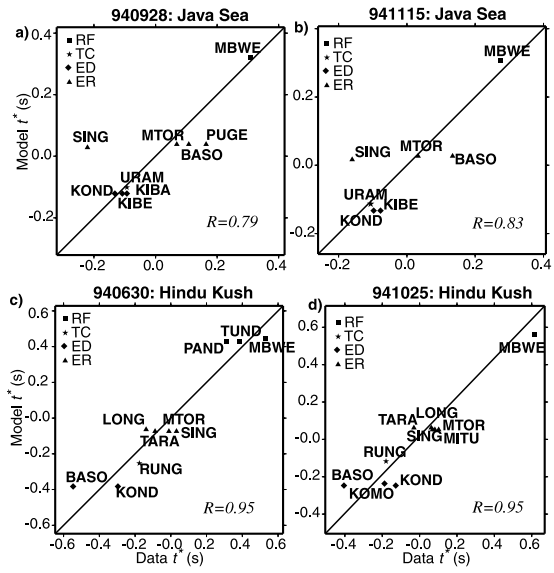

Figure 5. Comparison of model estimates of relative t^* with the relative t^* values determined from data for: a) 940928: Java Sea event; b) 941115: Java Sea event; c) 940630: Hindu Kush event; and d) 941025: Hindu Kush event. The correlation coefficients (R) are indicated on each plot.

seismic velocities seen in the models of *Ritsema et al.* [1998] and *Weeraratne et al.* [2003].

[13] Following *Karato* [1993], we express the dependence of P wave velocity variation on temperature in the upper mantle as:

$$\partial \ln V/\partial T = \partial \ln V_0/\partial T - F(\alpha)\left(Q^{-1}(\omega, T)/\pi\right)\left(H^*/RT^2\right) \quad (3)$$

where $\partial \ln V/\partial T$ is the observed velocity perturbation ($\partial \ln V$) with temperature change (∂T). The two terms on the right hand side of equation (3) are the elastic and anelastic contributions to the velocity perturbation, respectively. We assume $\partial \ln V_0/\partial \mathrm{T} \approx -5 \times 10^{-5}$ K^{-1} activation enthalpy $H^* \approx 500$ kJ/mol, and $T \approx 1600$ K, (all values from *Karato* [1993]), and $F(\alpha) = 1$ (constant Q). The P wave velocity anomaly in the RF region varies between -2% and -4% compared to the ED region [*Ritsema et al.*, 1998] which is to the east of the rift and has sublithospheric Q_P values similar to PREM at depths greater than 310 km. If the velocity anomaly beneath the rift is -2%, using $Q_P \approx 80$, and $\partial \ln V_P \approx -2\%$, we obtain $\partial T \approx 140$ K from equation (3). If the velocity anomaly beneath the rift is -4%, then $\partial \ln V_P \approx -4\%$, and $\partial T \approx 280$ K. Similar calculations for temperature beneath the craton cannot be performed because structure at these depths beneath the craton is poorly imaged in body wave studies.

5. Conclusions

[14] We conclude that the variation in Q_P within the sublithospheric mantle is sufficient to explain the observed t^* values for Tanzania. This finding is different from results for some other hotspots such as Iceland, where variation in t^* values could not be explained with simple Q models [*Allen et al.*, 1999]. By combining our Q_P models with estimates of velocity variations, we obtain a temperature anomaly of 140–280 K in the mantle beneath the eastern rift region. This finding is consistent with the results from *Owens et al.* [2000], who infer a temperature increase of 200–300 K in the eastern rift region from the depression in the 410 km discontinuity. Depending on the ambient mantle temperature, this temperature increase may or may not be sufficient to induce partial melting.

[15] How do these Q_P values compare with other studies in spreading regions? If we assume $Q_P \sim 9/4 Q_S$ [*Anderson*, 1989], the average rift Q_P values (~ 80) in our study are comparable to the Q_S values (~ 20 with 35) obtained by *Flanagan and Wiens* [1990] for the Lau back arc spreading center. Low values of Q_S (~ 50–70) are also obtained from studies of the east Pacific rise [*Webb and Forsyth*, 1998]. Thus, the decrease in attenuation observed beneath the eastern rift in Tanzania is consistent with other observations of low attenuation values close to spreading centers.

[16] **Acknowledgments.** AV is grateful to Greg Beroza for his continued support of her work. We thank Manika Prasad for helpful discussions and comments on the manuscript. We also thank two anonymous reviewers for their suggestions. This research was supported by the George A. Thompson Postdoctoral Fellowship sponsored by the Department of Geophysics and School of Earth Sciences at Stanford University.

References

Allen, R. M., et al. (1999), The thin hot plume beneath Iceland, *Geophys. J. Int.*, *137*, 51–63.

Anderson, D. L. (1989), *Theory of the Earth*, 366 pp., Blackwell Sci., Malden, Mass.

Brazier, R. A., A. A. Nyblade, and C. A. Langston (2000), Pn wave velocities beneath the Tanzania craton and adjacent rifted mobile belts, East Africa, *Geophys. Res. Lett.*, *27*(16), 2365–2368.

Cammarano, F., S. Goes, P. Vacher, and D. Giardini (2003), Inferring upper-mantle temperatures from seismic velocities, *Phys. Earth Planet. Sci.*, *138*(3–4), 197–222.

Dziewonski, A. M., and D. L. Anderson (1981), Preliminary reference Earth model, *Phys. Earth Planet. Inter.*, *25*, 297–356.

Flanagan, M. P., and D. A. Wiens (1990), Attenuation structure beneath the Lau back arc spreading center from teleseismic *S* phases, *Geophys. Res. Lett.*, *17*(12), 2117–2120.

Karato, S. (1993), Importance of anelasticity in the interpretation of seismic tomography, *Geophys. Res. Lett.*, *20*(15), 1623–1626.

Kennet, B. L. N., and E. R. Engdahl (1991), Travel times for global earthquake location and phase identification, *Geophys. J. Int.*, *105*, 429–465.

Langston, C. A., A. A. Nyblade, and T. J. Owens (2002), Regional wave propagation in Tanzania, East Africa, *J. Geophys. Res.*, *107*(B1), 2003, doi:10.1029/2001JB000167.

Last, R. J., A. A. Nyblade, C. A. Langston, and T. J. Owens (1997), Crustal structure of the East African plateau from receiver functions and Rayleigh wave phase velocities, *J. Geophys. Res.*, *102*(B11), 24,469–24,482.

Nyblade, A. A. (1997), Heat flow across the East African plateau, *Geophys. Res. Lett.*, *24*(16), 2083–2086.

Nyblade, A. A. (2002), Crust and upper mantle structure in East Africa: Implications for the origin of Cenozoic rifting and volcanism and the formation of magmatic rifted margins, in *Volcanic Rifted Margin*, edited by M. A. Menzies et al., *Spec. Pap. Geol. Soc. Am.*, *362*, 15–26.

Owens, T. J., A. A. Nyblade, and C. A. Langston (1995), The Tanzania broadband experiment, *Inc. Res. Inst. Seismol. Newslett.*, *14*, 1.

Owens, T. J., A. A. Nyblade, H. Gurrola, and C. A. Langston (2000), Mantle transition zone structure beneath Tanzania, East Africa, *Geophys. Res. Lett.*, *27*(6), 827–830.

Ritsema, J., A. A. Nyblade, T. J. Owens, C. A. Langston, and J. C. VanDecar (1998), Upper mantle seismic velocity structure beneath Tanzania, East Africa: Implications for the stability of cratonic lithosphere, *J. Geophys. Res.*, *103*(B9), 21,201–21,213.

VanDecar, J. C., and R. S. Crosson (1990), Determination of teleseismic relative phase arrival times using multi-channel cross-correlation and least squares, *Bull. Seismol. Soc. Am.*, *80*(1), 150–169.

Webb, S. C., and D. W. Forsyth (1998), Structure of the upper mantle under the EPR from waveform inversion of regional events, *Science*, *280*(5367), 1227, doi:10.1126/science.280.5367.

Weeraratne, D. S., D. W. Forsyth, K. M. Fischer, and A. A. Nyblade (2003), Evidence for an upper mantle plume beneath the Tanzanian craton from Rayleigh wave tomography, *J. Geophys. Res.*, *108*(B9), 2427, doi:10.1029/2002JB002273.

A. A. Nyblade, Department of Geosciences, Pennsylvania State University, University Park, PA, USA.

J. Ritsema, Laboratoire de Sismologie, Institut de Physique du Globe, Paris, France.

A. Venkataraman, Department of Geophysics, Stanford University, 397 Panama Mall, Mitchell Bldg., Stanford, CA 94305-2215, USA. (anupamav@pangea.stanford.edu)